Optofluidic pressure sensor based on interferometric imaging

Wuzhou Song* and Demetri Psaltis

Optics Laboratory, School of Engineering, Swiss Federal Institute of Technology Lausanne (EPFL), CH-1015 Lausanne, Switzerland

**Corresponding author: wuzhou.song@epfl.ch*

Received July 27, 2010; revised September 22, 2010; accepted September 28, 2010; posted October 5, 2010 (Doc. ID 132301); published October 21, 2010

We present a chip-scale optofluidic interferometric sensor for measuring liquid pressure based on an imaging method. The chip was constructed with a polymer by multilayer soft lithography. It consists of a flexible air gap optical cavity, which, upon illumination by monochromatic light, generates interference patterns that depend on pressure. The pressure was measured by imaging and analyzing the interference patterns. We also employed a pattern recognition algorithm that significantly simplified the calculation and enhanced the measurement reliability. This pressure sensor was demonstrated with a working range of 0–22 psi and an accuracy of ±1.4% of full scale when temperature stabilized. © 2010 Optical Society of America

OCIS codes: 120.5475, 120.3180, 160.5470, 130.3990.

Pressure sensors are widely used for controlling and monitoring thousands of everyday applications, while miniature pressure sensors have made substantial progress since the development of microfabrication techniques. Different types of miniature pressure sensors have been developed, such as piezoresistive, capacitive, and optical. Of particular relevance is the diaphragm-based Fabry–Perot (FP) interferometric fiber pressure sensor in which a tiny FP cavity is fabricated at the tip of the fiber and the pressure can be monitored from the reflected beam intensity [1,2]. However, the sophisticated fabrication process results in a high cost for such types of fiber pressure sensors. Thus, a low-cost and simply fabricated optical pressure sensor that can be directly integrated into microfluidic circuits would be desirable, especially as demand for single-use devices of lab-on-a-chip increases. In recent years, the combination of microfluidics and optics has led to the emerging field of optofluidics [3]. A variety of reconfigurable optofluidic devices have been demonstrated, such as the tunable lens [4] and laser sources [5–8]. Optofluidic methods make it possible to build optical components on a chip in the same way as we fabricate microfluidics. In this Letter, we present an optofluidic pressure sensor chip that was fabricated by multilayer soft lithography. The fluid pressure is measured by taking an image of the interference pattern formed upon illumination by a monochromatic light source.

Figure 1 shows the schematic of the whole pressure sensing apparatus, including the optofluidic pressure sensor chip and a camera. During measurement, the pressure force from the fluid causes deformation of the flexible membrane, hence the variation of the air-gap thickness. Upon illumination by monochromatic light, the reflected light from the air-gap boundaries interferes with each other constructively or destructively, depending on the air-gap thickness. The resulting total reflection intensity can be expressed as

$$I = I_1 + I_2 + 2\sqrt{I_1 I_2}\cos\left(\frac{4d\pi}{\lambda} + \pi\right), \qquad (1)$$

where I_1 and I_2 are the reflection intensity from the bottom and top polydimethylsiloxane (PDMS)–air boundaries, respectively; d is the air-gap distance. Assuming the incident intensity is I_0 due to the low reflectivity on these two boundaries, we have $I_1 \approx I_2 \approx I_0 \times 4\%$. Multiple reflections can be neglected in this case. The fact that $I_1 \approx I_2$ ensures good image contrast of the interference patterns. As the air-gap chamber has a round shape, the PDMS membrane is deformed to a dome shape upon applied pressure. The multiple concentric interference rings are similar to the Newton ring pattern. This interference pattern was captured by the CCD camera through the objective lens.

The top and bottom PDMS slabs were replicated from two different master molds, which are defined by the negative photoresist SU-8 on silicon wafers. The middle PDMS membrane was made by spinning multiple layers of PDMS on a flat silicon wafer. All the characterization in this Letter is based on chips with a membrane thickness of 537 μm unless otherwise stated. As shown in

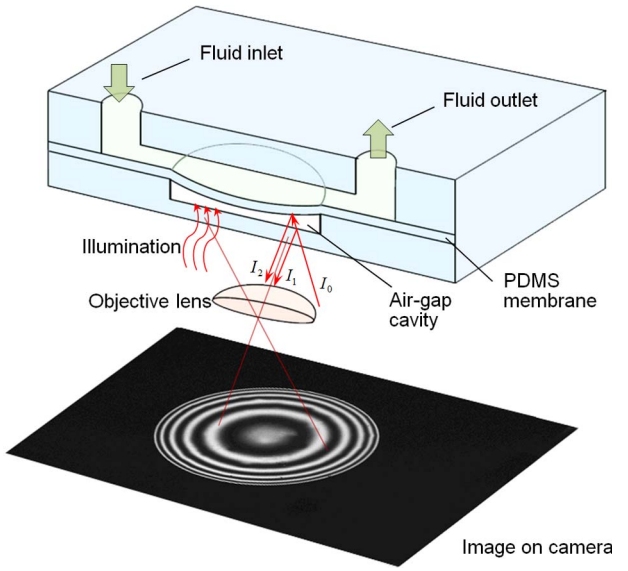

Fig. 1. (Color online) Schematic of the pressure sensing apparatus including the chip and an imaging device.

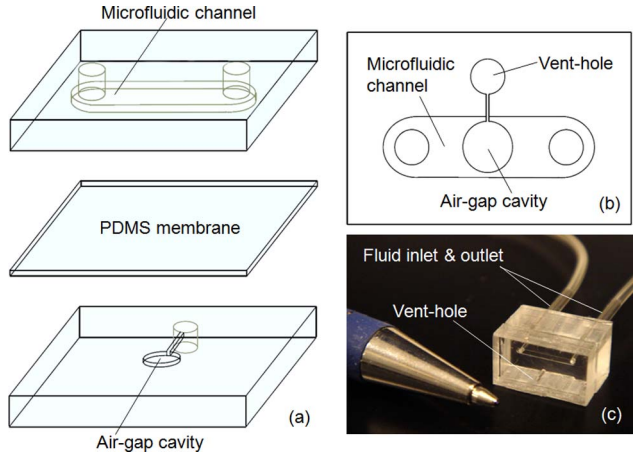

Fig. 2. (Color online) (a) Structure of the chip, (b) top view of the chip structures, and (c) picture of the optofluidic chip.

Fig. 2(a), the three parts were finally aligned and bonded together using an oxygen plasma treatment. Figure 2(b) shows the top view of the chip structure. The dimensions of the air-gap cavity are 400 μm diameter and 15 μm thickness. The air-gap cavity connects to the atmosphere through the vent hole for keeping constant pressure in the air gap. The microfluidic channel has a width of 600 μm and a thickness of 50 μm. A picture of the fabricated device is shown in Fig. 2(c). The interference patterns from the chip were measured on a bright-field microscope with a built-in beam splitter for illumination. We used a diffusive monocolor light source, which includes a tungsten light source and a laser line filter (Thorlabs, FL632.8-1) with a transmission linewidth of 1 nm. We found that this monochromatic light source has sufficient temporal coherence for generating high-quality interference patterns without speckle noise. The pressure was calibrated with a digital pressure gauge. Figure 3(a) shows an example image of the interference pattern captured at a pressure of 3.80 psi. The background area outside the air-gap cavity is dark owing to

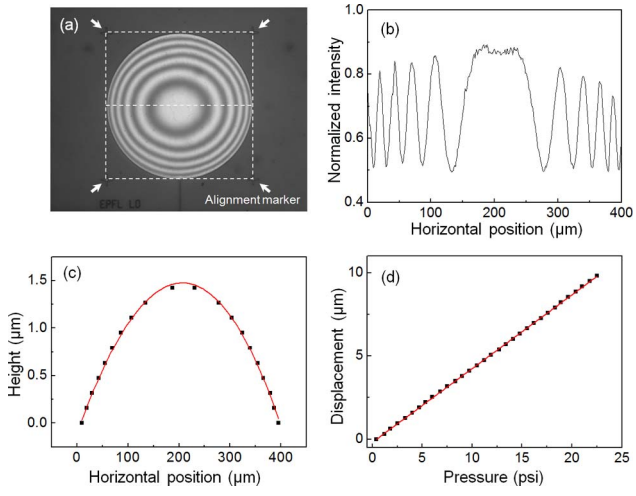

Fig. 3. (Color online) (a) Example image of the interference pattern at 3.80 psi. The square of the dashed line indicates the correlation area. (b) Intensity profile of the area indicated by the dashed line in the middle of Fig. 3(a). (c) Corresponding surface profile of the membrane. (d) Plot of displacement of membrane in center versus the pressure.

the low reflectivity at the PDMS–water interface, where the contrast of the refractive indices (1.41:1.33) is much lower than that of PDMS–air (1.41:1).

To calculate the pressure value from the recorded interference patterns, we adopted an image correlation method to analyze the holographic fringes. We use the Pearson correlation coefficient to characterize the similarity between two (gray scale) images, as described by the following equation:

$$r = \frac{\sum_i (A_i - A_m)(B_i - B_m)}{\sqrt{\sum_i (A_i - A_m)^2}\sqrt{\sum_i (B_i - B_m)^2}}, \quad (2)$$

where A_i is the intensity of the ith pixel in image A, B_i is the intensity of the ith pixel in image B, A_m is the mean intensity of image A, and B_m is the mean intensity of image B. Before measurement, the pressure sensor was calibrated with the digital gauge from 0 to 22 psi at 0.1 psi intervals. As the intensity of each pixel on the image varies continuously in terms of pressure, it is possible to add many more reference images by interpolating from the nearby reference images. The interpolation significantly alleviates the calibration work while enhancing the measuring resolution. After interpolation, the total number of reference images was increased by ten times from the original one. In Fig. 3(a) the dashed square indicates the area over which the image correlation was calculated, and the corresponding intensity profile is plotted in Fig. 3(b). The relative heights of each of the peak positions were calculated. The results are plotted in squares in Fig. 3(c). The red curve in Fig. 3(c) is the fitting curve, which gives the profile of the membrane surface. Figure 3(d) is the plot of displacement of the membrane in the center area versus the pressure. It turns out to be very nicely linearly related. From the slope, the pressure sensitivity is calculated to be 0.444 μm/psi. The measurement results at 12 different

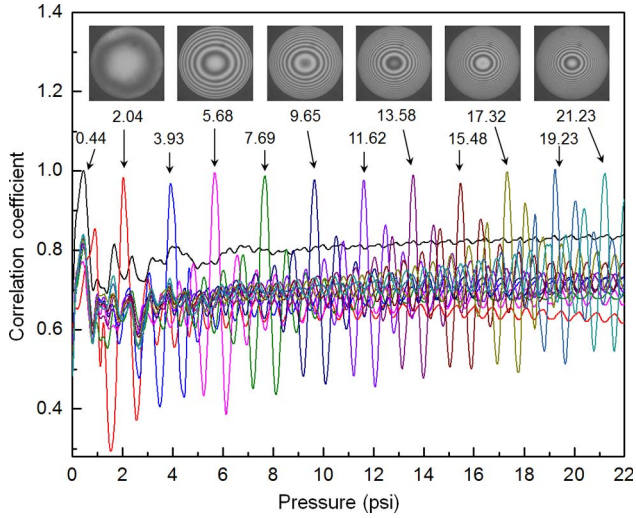

Fig. 4. (Color online) Plot of the correlation coefficient against the pressure of reference images. The different colors correspond to different measurement points. The insets show the recorded images at the corresponding pressures. The numbers are the measured pressure values obtained from the horizontal position of these maximum peaks.

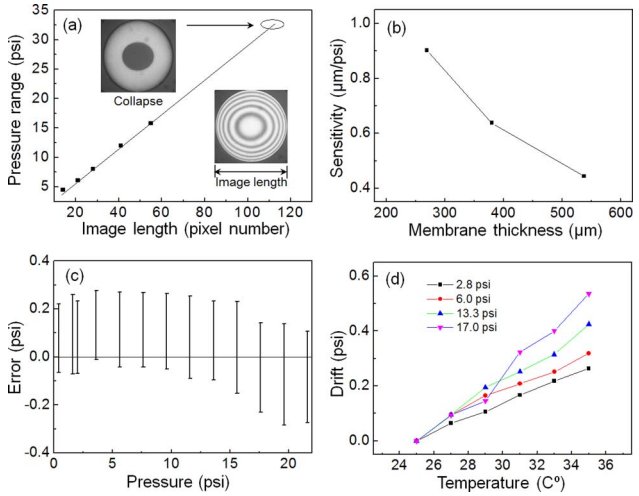

Fig. 5. (Color online) (a) Simulated result of the dependence of the upper limit working range on the image length. (b) Relation between the pressure sensitivity and the membrane thickness. (c) Distribution of the pressure error at different pressures. (d) Drift of measurement value with temperature at different pressure conditions.

pressure points in the range of 0–22 psi are shown in Fig. 4, where the horizontal coordinate represents the pressure value of each of the reference images, and the vertical coordinate represents the correlation coefficient between the measuring image and the reference images. The area for imaging correlation is indicated by the square of dashed lines in Fig. 3(a). Thus, the measured pressure is determined by the x coordinate of the maximum peak on the plot of the correlation coefficient against the pressure of references.

The working range of this device is limited to above 0 psi. We found that, even at very low pressure, the interference pattern becomes almost flat without fringes; the image correlation method is still effective and accurate. The upper limit of the working range can extend to 32 psi, at which point the membrane begins to touch the other side of the cavity, as shown in the left inset of Fig. 5(a) at the pressure of 33 psi. Another possible factor that limits the working range is the image resolution of the correlation area. When the pressure is too high, the fringes become too dense and the camera can no longer distinguish them. We have stimulated different image sizes of the correlation area. Figure 5(a) shows the relation between the image length and the upper limit of the working range. As the original image length of the correlation area is 542 pixels, we can find that such an image size is sufficient for the working range of 0–32 psi. For a given air-gap thickness, the working range can be changed by adjusting the thickness of the PDMS membrane. Figure 5(b) shows the dependence of the pressure sensitivity on the membrane thickness. Although the working range of this pressure sensor can be extended to 32 psi, we demonstrated only the working range of 0–22 psi. At each pressure condition, the measurements were repeated at least five times, based on a different previous state. Figure 5(c) shows the error bar in the working range of 0–22 psi. The pressure accuracy is about $\pm 1.4\%$ of full scale. During the measurement we found that the pressure error is related to the previous state. This was interpreted as the result of the shape memory effect of the PDMS membrane. The temperature effect on the pressure accuracy is also significant, as shown in Fig. 5(d). All the measured values at different pressure conditions have an increasing tendency with increasing temperature.

In conclusion, we demonstrated a low-cost, image-based interferometric optofluidic pressure sensor on a polymer chip. Rather than using the research microscope and camera to measure the interference patterns, as we did in this prototyping work, we believe a much cheaper external monitoring device can be constructed with plastic optics components, an LED light source, and a webcam-type camera.

References

1. X. Wang, J. Xu, Y. Zhu, K. L. Cooper, and A. Wang, Opt. Lett. **31**, 885 (2006).
2. Y. Kim and D. P. Neikirk, IEEE Photon. Technol. Lett. **7**, 1471 (1995).
3. D. Psaltis, S. R. Quake, and C. Yang, Nature **442**, 381 (2006).
4. C. Song, N.-T Nguyen, A. K. Asundi, and C. Lee-Ngo Low, Opt. Lett. **34**, 3622 (2009).
5. W. Song and D. Psaltis, Appl. Phys. Lett. **96**, 081101 (2010).
6. Y. Cheng, K. Sugioka, and K. Midorikawa, Opt. Lett. **29**, 2007 (2004).
7. W. Song, A. E. Vasdekis, Z. Li, and D. Psaltis, Appl. Phys. Lett. **94**, 051117 (2009).
8. W. Song, A. E. Vasdekis, Z. Li, and D. Psaltis, Appl. Phys. Lett. **94**, 161110 (2009).